

Characterization of Pd···H-C interactions in *bis*-dimethyldithiocarbamate palladium(II) and its deuterated analog by luminescence spectroscopy at variable pressure

Stéphanie Poirier, Elodie Tailleur, Hudson Lynn, Christian Reber*

Département de chimie, Université de Montréal, Montréal, Québec, H3C 3J7, Canada.

Table of contents

Synthesis and characterization	2
Table S1. Variable-pressure slopes of absorption or luminescence maxima for d-d transitions as reported in the literature. Complexes in italics are used to calculate the average $\Delta E_{\max}/\Delta P$ value for d ⁸ square-planar complexes with chelating ligands.....	4
Table S2. Crystallographic data for [Pd{(CD ₃) ₂ DTC} ₂] and [Pd{((CH ₃) ₂ DTC) ₂ }]	6
Table S3. Selected bond distances, angles, intermolecular distances and intermolecular angles for [Pd{((CH ₃) ₂ DTC) ₂ } and [Pd{(CD ₃) ₂ DTC} ₂].....	7
Figure S1. Packing and M···H-C interaction (red) in the crystal structure.....	8
Figure S2. Raman spectra of [Pd{((CH ₃) ₂ DTC) ₂ } at variable pressure.....	9
Figure S3. Raman spectra of [Pd{(CD ₃) ₂ DTC} ₂] at variable pressure.....	9
Figure S4. Evolution of Raman shifts with pressure for [Pd{((CH ₃) ₂ DTC) ₂ }]. The C-H modes are enlarged in the top figure. Dotted lines outline pressure regions where changes occur in luminescence spectroscopy.	10
Figure S5. Evolution of Raman shifts with pressure for [Pd{(CD ₃) ₂ DTC} ₂ }]. The C-D modes are enlarged in the top figure. Dotted lines outline pressure regions where changes occur in luminescence spectroscopy.	11
Figure S6. Superposition of calculated (black) and experimental (red) Raman spectra of [Pd{(CD ₃) ₂ DTC} ₂].	12
Figure S7. Superposition of calculated (black) and experimental (red) Raman spectra of [Pd{((CH ₃) ₂ DTC) ₂ }].	12

Synthesis and characterization

The synthesis, characterization and crystal structure of $[Pd\{(CH_3)_2DTC\}_2]$ are published.¹ Elemental analysis calculated for $S_4N_2C_6H_{14}Pd$ (346.86): S 36.76, N 8.03, C 20.66, and H 4.04; found: S 36.86, N 7.78, C 20.93, and H 3.82. Vibrational frequencies (Raman, cm^{-1}): 271 (w), 326 (vs), 385 (s), 417 (s), 553 (w), 572 (vs), 896(s), 964 (s), 1013 (w), 1049 (w), 1100 (w), 1145 (m), 1242 (w), 1394 (s), 1447 (m) and 1552 (m).

Synthesis of $[Pd\{(CD_3)_2DTC\}_2]$. 0.1095 g (0.51 mmol) of hydrated $PdCl_2$ were dissolved in a minimum (175 mL) of dimethylsulfoxide (DMSO). Two equivalents (0.1053 g, 1.20 mmol) of anhydrous deuterated dimethylamine ($NH(CD_3)_2 \cdot HCl$) were dissolved in a minimum (25 mL) of ethanol 95 %. Four equivalents (0.0936 g, 2.34 mmol) of sodium hydroxide (NaOH) were dissolved in a minimum (40 mL) of ethanol 95% and added to an excess of carbon disulfide (0.5 mL, 8.3 mmol). The solutions of dimethylamine and sodium hydroxide were mixed, forming the deuterated sodium dimethyldithiocarbamate ($NaCD_3DTC$). The deuterated dimethyldithiocarbamate solution and metal solution were combined, giving an orange powder. The powder was filtered, washed with diethyl ether and collected with a yield of 23%. Yield was calculated from the molar ratio of the obtained complex and the initial palladium(II) salt. Single crystals were obtained by recrystallization in acetone. Vibrational frequencies (Raman, cm^{-1}): 242 (w), 318 (s), 350 (s), 398 (s), 540 (vs), 794 (m), 837 (w), 943 (m), 970 (s), 980 (sh.), 1036 (sh.), 1054 (m), 1118 (w), 1226 (w) and 1496 (s).

X-ray crystallography. Single crystals of $C_6D_{12}N_2PdS_4$ and $C_6H_{12}N_2PdS_4$ were collected with a Bruker Venture Metaljet diffractometer. The crystals were kept at 295 K during data collection. Using Olex2,² the structures were solved with the XT³ structure solution program using Direct Methods and refined with the XL⁴ refinement package using Least Squares minimisation.

Luminescence and Raman spectroscopy. Luminescence and Raman spectra of $[Pd\{(CH_3)_2DTC\}_2]$ and $[Pd\{(CD_3)_2DTC\}_2]$ were measured using an InVia spectrometer coupled to an imaging microscope (Leica) and argon ion lasers. The excitation wavelengths used were 488 nm for all luminescence measurements and also for Raman spectra of $[Pd\{(CH_3)_2DTC\}_2]$, and 785 nm for Raman spectra of $[Pd\{(CD_3)_2DTC\}_2]$. Pressure was applied by a gasketed diamond-anvil cell (DAC, High-Pressure Diamond Optics). The crystals are loaded in the gasket in a Nujol oil medium, for pressure-transmitting. Ruby is also added in the gasket to calibrate the pressure.⁵ All spectra were corrected by calibration with a tungsten lamp to adjust for system response.

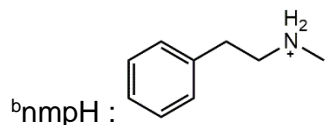
Calculated Raman spectra. Superposition of experimental and calculated Raman spectra is presented in Fig.S6 and S7. The good agreement highlights the phase purity. All DFT calculations were performed with the Gaussian09 software⁶ (Revision D.01, Gaussian Inc.) and the calculation results were visualized and presented using the 5.08 release of the GaussView software (Gaussian Inc.). Initially, a ground-state geometry optimization was carried out for the compound $[\text{Pd}(\{\text{CH}_3\}_2\text{DTC})_2]$ and its deuterated analogue $[\text{Pd}(\{\text{CD}_3\}_2\text{DTC})_2]$ in the gas-phase using the geometric parameters (bond lengths, angles and dihedral angles) of a single complex taken from their respective crystal structure.¹ This optimization was accomplished with the hybrid exchange-correlation functional B3LYP^{7, 8} along with the relativistic basis set Lanl2dz⁹ for Pd, the 6-31+G* basis set for S and the 6-31G basis set for C, H and N. The obtained optimized structures were used subsequently for a frequency calculation at the same level of theory to yield the calculated Raman spectra with an arbitrary full width at half maximum of 4 cm⁻¹ for the calculated vibrational transitions. No imaginary frequencies were observed, confirming that the obtained optimized structures correspond to energy minima.

Table S1. Variable-pressure slopes of absorption or luminescence maxima for d-d transitions as reported in the literature. Complexes in italics are used to calculate the average $\Delta E_{\max}/\Delta P$ value for d⁸ square-planar complexes with chelating ligands.

Complexes	Range of linearity (kbar)	$\Delta E_{\max}/\Delta P$ (cm ⁻¹ /kbar)	Ref
Octahedral geometry			
[Ni(NH ₃) ₆]Cl ₂	0 - 70	+20	10, 11
[Ni(H ₂ O) ₆]SO ₄	0 - 70	+20	11
NiO	0 - 100	+8	12, 13
NiCl ₂	0 - 90	+12	10
NiBr ₂	0 - 60	+15	10
CoCl ₂	0 - 100	+13	10
CoBr ₂	0 - 60	+12	10
Al ₂ O ₃ :Ti ³⁺ , Al ₂ O ₃ :V ³⁺ , Al ₂ O ₃ :Ni ²⁺ , Al ₂ O ₃ :Ni ³⁺ , Al ₂ O ₃ :Cr ³⁺	0 - 50	+10	14, 15
MgO :Ti ³⁺ , MgO :Ni ²⁺ , MgO :Cr ³⁺ , MgO :Co ²⁺	0 - 90	+10 to +20	15
Distorted tetrahedral geometry			
[GuH] ₄ [Cu ₂ (cit) ₂]·2H ₂ O ^a	0 - 65	+10 to +14	16
Square-planar geometry			
(nmpH) ₂ [CuCl ₄] ^b	0 - 40	+17	17
(NbzipzH ₂ Cl) ₂ [CuCl ₄]	0 - 30	+30	17, 18
(BF ₄) ₂ [Cu(dieten) ₂] ^c	0 - 50	+15	17
[Ni(HSaloxF) ₂] ^d	0 - 60		19
[Ni(HSaloxMeO) ₂] ^e	0 - 60		19
(n-Bu ₄ N) ₂ [Pd(SCN) ₄]	0 - 30	+29	20
(n-Bu ₄ N) ₂ [Pd(SeCN) ₄]	0 - 30	+25 ± 2	20
[Pd(EDTC) ₂] ^f	0 - 50	+9	21
[Pd(PDTC) ₂] ^g	0 - 50	+13	21
[Pd{PyCHC(C ₃ F ₇)O} ₂]	0 - 25	+13 ± 2	22
[Pd{PyCHC(CH ₃)O} ₂]	0 - 25	-15 ± 7	22
[Pd(ttcn)Cl ₂] ^h	0 - 30	+6	23
(n-Bu ₄ N) ₂ [Pt(SCN) ₄]	0 - 30	+24	20
(n-Bu ₄ N) ₂ [Pt(SeCN) ₄]	0 - 30	+12	20

$K_2[PtCl_4]$	0 - 57	+20	^{24, 25}
$K_2[Pt(SCN)_4]$	0 - 57	+10 ± 3	²⁵
$[Pt(dopDTC)_2]^f$	0 - 50	+11 ± 1	²⁶
$[Pt(EDTC)_2]^f$	0 - 30	+15	²¹
$[Pt\{(CH_3)_2DTC\}_2]$	0 - 40	+47 ± 3	²⁶
$[Pt(SCN)_2\{(\mu-SCN)Mn(NCS)(bipy)_2\}_2]$	0 - 35	-99 ± 6	²⁷
$[Pt(ttcn)Cl_2]^h$	0 - 30	-20	²³

^aGuH: Guanidinium cation, H₄cit:citric acid.



^cdieten : *N,N'*-diethylethylenediamine

^dHSaloxF: 3-fluorosalicylaldoxime

^eHSaloxMeO: 3-methoxysalicylaldoxime

^fEDTC : diethyldithiocarbamate

^gPDTC : pyrrolidine-*N*-dithiocarbamate

^httcn : 1,4,7-trithiacyclononane

ⁱdopDTC : di(o-pyridyl)-dithiocarbamate

Table S2. Crystallographic data for [Pd{((CD₃)₂DTC)₂} and [Pd{((CH₃)₂DTC)₂}]

Empirical formula	C ₆ D ₁₂ N ₂ PdS ₄	C ₆ H ₁₂ N ₂ PdS ₄
M (g mol ⁻¹)	358.89	346.82
System	triclinic	triclinic
Space group	P-1	P-1
T (K)	295	295
a (Å)	6.475(1)	6.482(2)
b (Å)	7.039(2)	7.034(2)
c (Å)	7.680(2)	7.680(2)
α (°)	65.235(6)	65.47(2)
β (°)	67.183(7)	66.92(2)
γ (°)	84.974(7)	84.65(2)
V (Å ³)	291.8(1)	292.0(2)
Z	1	1
ρ _{calcd.} (g cm ⁻³)	2.042	1.972
μ (mm ⁻¹)	12.709	12.699
Crystal size (mm ³)	0.32 × 0.24 × 0.06	0.08 × 0.04 × 0.03
Index ranges	-8 ≤ h ≤ 8 -9 ≤ k ≤ 9 -9 ≤ l ≤ 9	-8 ≤ h ≤ 8 -9 ≤ k ≤ 9 -9 ≤ l ≤ 9
F (000)	172.0	172.0
2Θ range (°)	12.096 to 121.652	11.968 to 121.302
Reflexions collected	5927	5153
Independent reflections	1289	1311
R _{int} (%)	5.43	4.25
Data/restraints/parameters	1289/0/64	1311/0/63
GoF ^a on F ²	1.264	1.027
R ₁ ^b [I >= 2σ(I)] (%)	5.23	2.80
wR ₂ ^c (all data) (%)	11.90	6.81
Largest diff. peak/hole (e Å ⁻³)	0.99/-1.14	0.54/-0.45

^aGoF = {Σ[F_o²-F_c²)²]/(n-p)}^{1/2}, where n is the number of reflections and p is the total number of parameters refined.

^bR1 = Σ||F_o|-|F_c||/Σ|F_o|.

^cwR₂ = {Σ[w(F_o²-F_c²)²]/Σ[w(F_o²)²]}^{1/2}.

Table S3. Selected bond distances, angles, intermolecular distances and intermolecular angles for $[\text{Pd}\{(\text{CH}_3)_2\text{DTC}\}_2]$ and $[\text{Pd}\{(\text{CD}_3)_2\text{DTC}\}_2]$.

$[\text{Pd}\{(\text{CH}_3)_2\text{DTC}\}_2]$		$[\text{Pd}\{(\text{CD}_3)_2\text{DTC}\}_2]$	
Bond distances			
Bond	Distance (\AA)	Bond	Distance (\AA)
Pd-S1	2.337(1)	Pd-S1	2.333(1)
Pd-S2	2.309(1)	Pd-S2	2.309(1)
S1-C3	1.718(3)	S1-C3	1.721(4)
S2-C3	1.725(3)	S2-C3	1.723(4)
C3-N1	1.323(4)	C3-N1	1.303(5)
N1-C1	1.457(4)	N1-C1	1.462(5)
N1-C2	1.457(4)	N1-C2	1.456(5)
Angles ($^\circ$)			
S1-Pd-S2	75.53(4)	S1-Pd-S2	75.73(4)
S2-Pd-S1	104.47(4)	S2-Pd-S1	104.27(4)
C1-N1-C2	115.9(3)	C1-N1-C2	116.4(3)
Intermolecular distances			
Pd-H2B	2.92	Pd-D2C	2.92
Pd-H1B	3.56	Pd-D1A	3.60
Pd-C2	3.81	Pd-C2	3.83
Pd-C1	4.31	Pd-C1	4.34
Pd-N1	4.18	Pd-N1	4.20
Intermolecular angles			
Pd-H2B-C2	155	Pd-D2C-C2	157
Pd-H1B-C1	137	Pd-D1A-C1	140

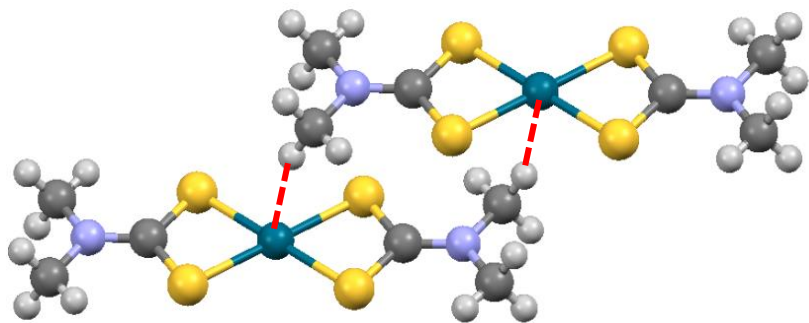


Figure S1. Packing and M···H-C interaction (red) in the crystal structure.

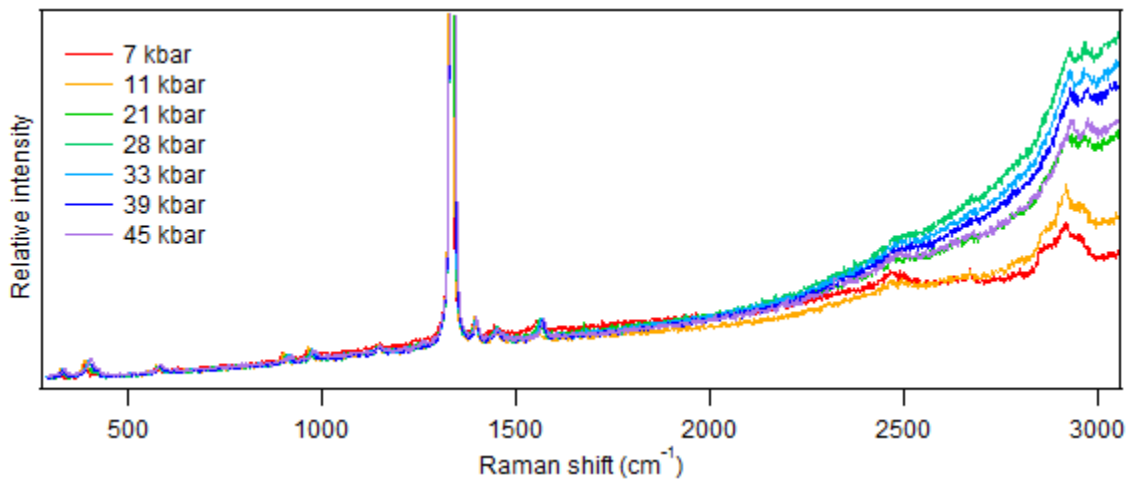


Figure S2. Raman spectra of $[\text{Pd}\{(\text{CH}_3)_2\text{DTC}\}_2]$ at variable pressure.

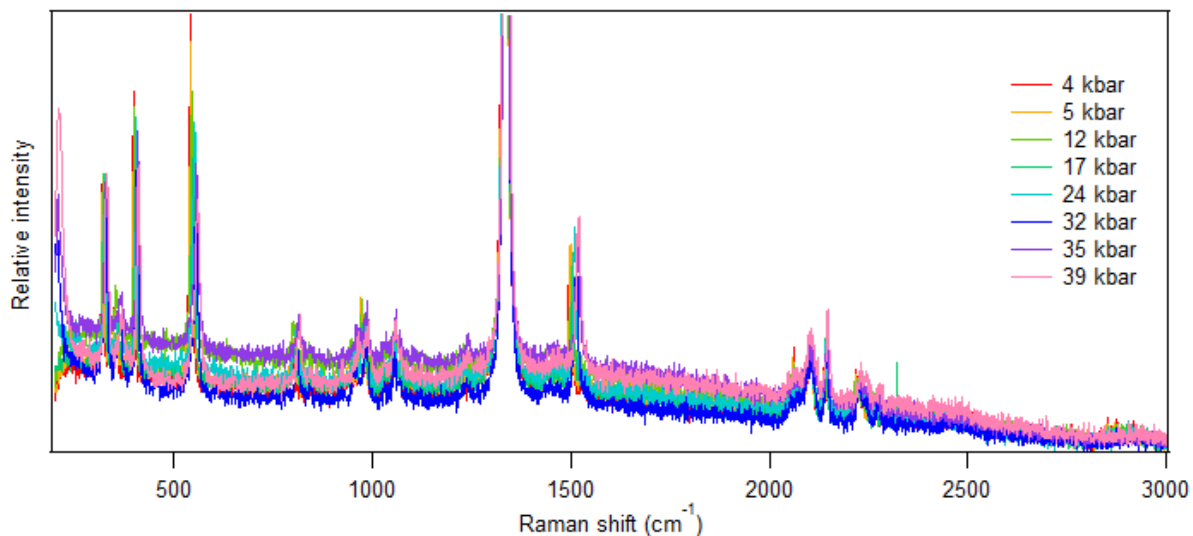


Figure S3. Raman spectra of $[\text{Pd}\{(\text{CD}_3)_2\text{DTC}\}_2]$ at variable pressure.

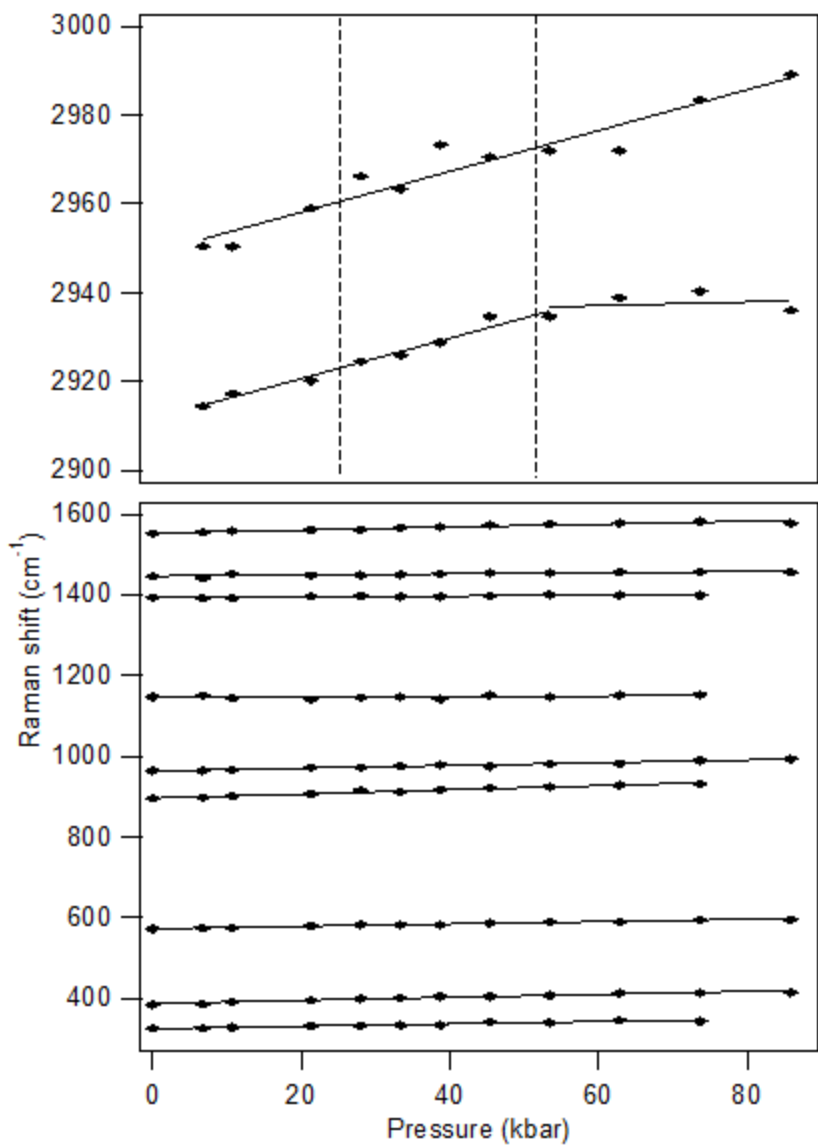


Figure S4. Evolution of Raman shifts with pressure for $[\text{Pd}(\text{CH}_3)_2\text{DTC}]_2$. The C-H modes are enlarged in the top figure. Dotted lines outline pressure regions where changes occur in luminescence spectroscopy.

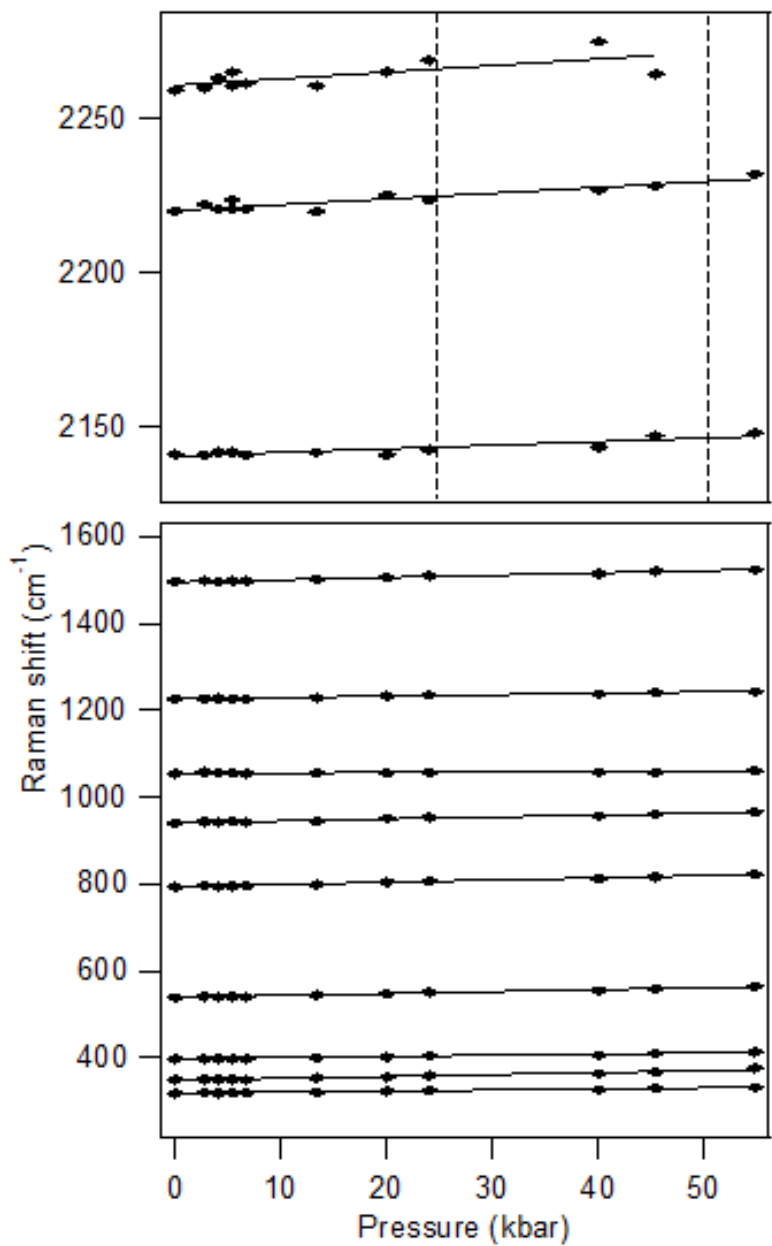


Figure S5. Evolution of Raman shifts with pressure for $[\text{Pd}\{(\text{CD}_3)_2\text{DTC}\}_2]$. The C-D modes are enlarged in the top figure. Dotted lines outline pressure regions where changes occur in luminescence spectroscopy.

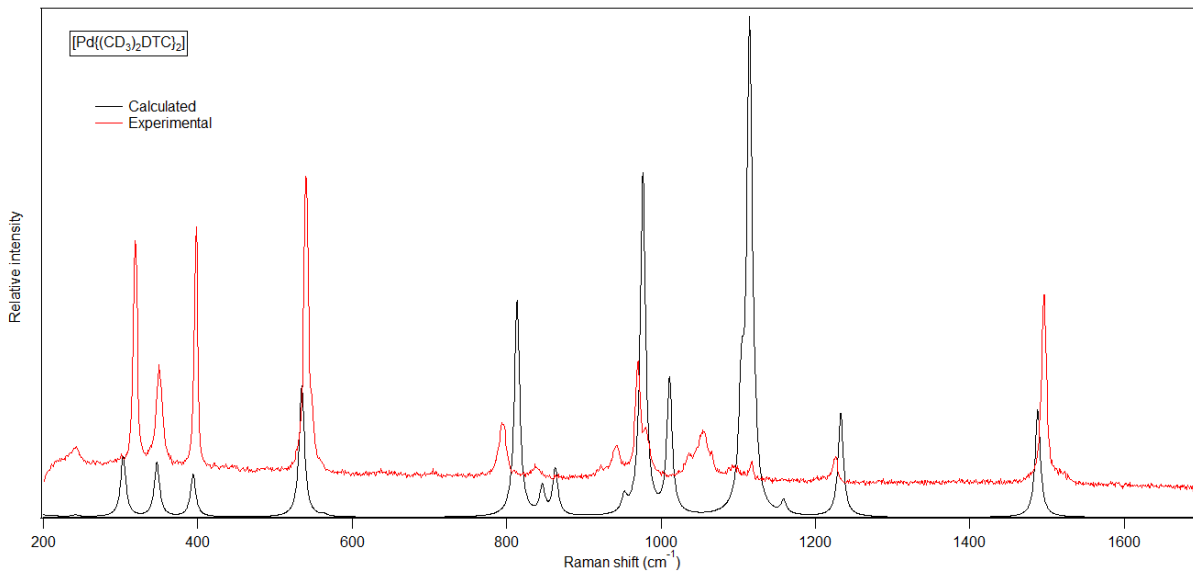


Figure S6. Superposition of calculated (black) and experimental (red) Raman spectra of $[\text{Pd}((\text{CD}_3)_2\text{DTC})_2]$.

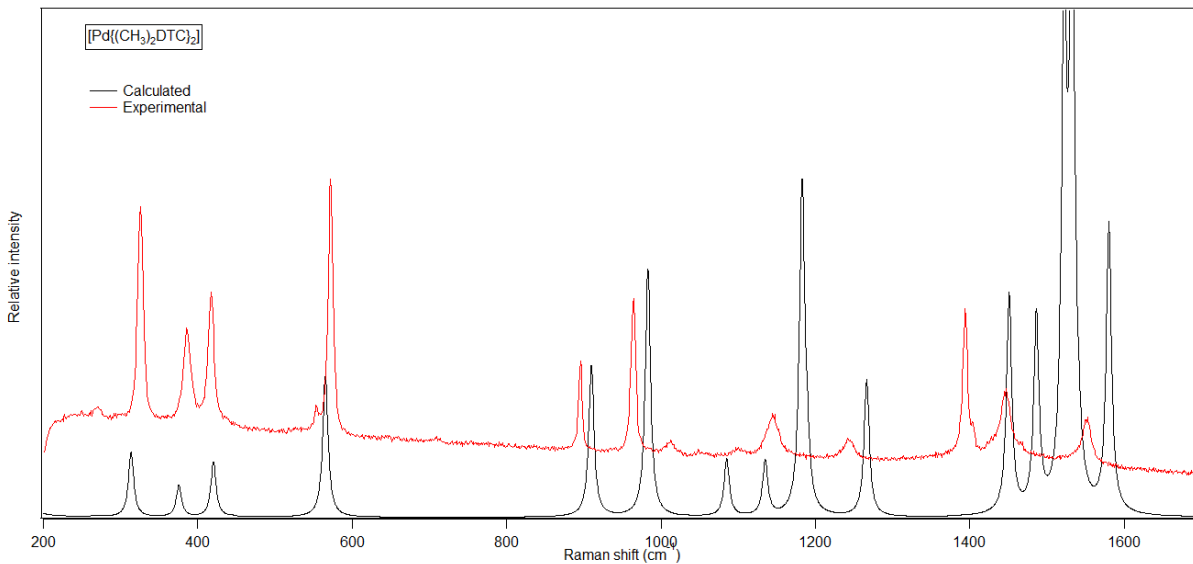


Figure S7. Superposition of calculated (black) and experimental (red) Raman spectra of $[\text{Pd}((\text{CH}_3)_2\text{DTC})_2]$.

References

1. S. Poirier, P. Guionneau, D. Luneau and C. Reber, *Can. J. Chem.*, 2014, **92**, 958-965.
2. O. V. Dolomanov, L. J. Bourhis, R. J. Gildea, J. A. K. Howard and H. Puschmann, *J. Appl. Crystallogr.*, 2009, **42**, 339-341.
3. G. M. Sheldrick, *Acta Crystallogr. C*, 2015, **71**, 3-8.
4. G. M. Sheldrick, *Acta. Crystallogr. A*, 2008, **64**, 112-122.
5. G. J. Piermarini, S. Block, J. D. Barnett and R. A. Forman, *J. Appl. Phys.*, 1975, **46**, 2774.
6. M. J. Frisch, G. W. Trucks, H. B. Schlegel, G. E. Scuseria, M. A. Robb, J. R. Cheeseman, G. Scalmani, V. Barone, B. Mennucci, G. A. Petersson, H. Nakatsuji, M. Caricato, X. Li, H. P. Hratchian, A. F. Izmaylov, J. Bloino, G. Zheng, J. L. Sonnenberg, M. Hada, M. Ehara, K. Toyota, R. Fukuda, J. Hasegawa, M. Ishida, T. Nakajima, Y. Honda, O. Kitao, H. Nakai, T. Vreven, J. A. J. Montgomery, J. E. Peralta, F. Ogliaro, M. Bearpark, J. J. Heyd, E. Brothers, K. N. Kudin, V. N. Staroverov, T. Keith, R. Kobayashi, J. Normand, K. Raghavachari, A. Rendell, J. C. Burant, S. S. Iyengar, J. Tomasi, M. Cossi, N. Rega, J. M. Millam, M. Klene, J. E. Knox, J. B. Cross, V. Bakken, C. Adamo, J. Jaramillo, R. Gomperts, R. E. Stratmann, O. Yazyev, A. J. Austin, R. Cammi, C. Pomelli, J. W. Ochterski, R. L. Martin, K. Morokuma, V. G. Zakrzewski, G. A. Voth, P. Salvador, J. J. Dannenberg, S. Dapprich, A. D. Daniels, O. Farkas, J. B. Foresman, J. V. Ortiz, J. Cioslowski and D. J. Fox, *Gaussian 09*, 2013.
7. A. D. Becke, *J. Chem. Phys.*, 1993, **98**, 5648.
8. J. Tirado-Rives and W. L. Jorgensen, *J. Chem. Theory Comput.*, 2008, **4**, 297-306.
9. P. J. Hay and W. R. Wadt, *J. Chem. Phys.*, 1985, **82**, 270-283.
10. J. C. Zahner and H. G. Drickamer, *J. Chem. Phys.*, 1961, **35**, 1483.
11. R. W. Parsons and H. G. Drickamer, *J. Chem. Phys.*, 1958, **29**, 930.
12. R. L. Clendenen and H. G. Drickamer, *J. Chem. Phys.*, 1966, **44**, 4223.
13. D. R. Stephens and H. G. Drickamer, *J. Chem. Phys.*, 1961, **34**, 937.
14. H. G. Drickamer, *Ber. Bunsenges. Phys. Chem.*, 1966, **70**, 952-957.
15. S. Minomura and H. G. Drickamer, *J. Chem. Phys.*, 1961, **35**, 903.
16. K. W. Galloway, S. A. Moggach, P. Parois, A. R. Lennie, J. E. Warren, E. K. Brechin, R. D. Peacock, R. Valiente, J. González, F. Rodríguez, S. Parsons and M. Murrie, *Cryst. Eng. Comm.*, 2010, **12**, 2516.
17. H. G. Drickamer and K. L. Bray, *Acc. Chem. Res.*, 1990, **23**, 55-61.
18. K. L. Bray and H. G. Drickamer, *J. Phys. Chem.*, 1990, **94**, 2154-2159.
19. P. J. Byrne, P. J. Richardson, J. Chang, A. F. Kusmartseva, D. R. Allan, A. C. Jones, K. V. Kamenev, P. A. Tasker and S. Parsons, *Chem. Eur. J.*, 2012, **18**, 7738-7748.
20. J. K. Grey, I. S. Butler and C. Reber, *Inorg. Chem.*, 2003, **42**, 6503-6518.
21. C. Genre, G. Levasseur-Thériault and C. Reber, *Can. J. Chem.*, 2009, **87**, 1625-1635.
22. S. Poirier, L. Czympiel, N. Belanger-Desmarais, S. Mathur and C. Reber, *Dalton Trans.*, 2016, **45**, 6574-6581.
23. E. Pierce, E. Lanthier, C. Genre, Y. Chumakov, D. Luneau and C. Reber, *Inorg. Chem.*, 2010, **49**, 4901-4908.
24. D. M. Preston, W. Guentner, A. Lechner, G. Gliemann and J. I. Zink, *J. Am. Chem. Soc.*, 1988, **110**, 5628-5633.
25. I. Hidvegi, W. Tuszynski and G. Gliemann, *Chem. Phys. Lett.*, 1981, **77**, 517-519.
26. S. Poirier, R. J. Roberts, D. Le, D. B. Leznoff and C. Reber, *Inorg. Chem.*, 2015, **54**, 3728-3735.
27. G. Levasseur-Thériault, C. Reber, C. Aronica and D. Luneau, *Inorg. Chem.*, 2006, **45**, 2379-2381.